

# Report of a Comparison between the LNE-LNHB and the BIPM of Absorbed Dose to Graphite in a Co-60 Reference Beam

S. Picard<sup>1</sup>, D. T. Burns<sup>1</sup>, C. Kessler<sup>1</sup>, P. Roger<sup>1</sup>,  
F. Delaunay<sup>2</sup>, J. Daures<sup>2</sup>, M. Donois<sup>2</sup> and A. Ostrowsky<sup>2</sup>

<sup>1</sup>Bureau International des Poids et Mesures

<sup>2</sup>Laboratoire National Henri Becquerel



February 2015

## Abstract

A comparison of absorbed dose to graphite in a Co-60 reference beam was carried out between the Laboratoire National de Métrologie et d'Essais – Laboratoire National Henri Becquerel (LNE-LNHB) and the Bureau International des Poids et Mesures (BIPM) in March 2011. The comparison involved the LNE-LNHB primary standard graphite calorimeter and the BIPM graphite calorimeter used for the BIPM.RI(I)-K6 comparison of national accelerator beam facilities. The comparison result, reported as a ratio of the LNE-LNHB and the BIPM evaluations, is 0.992 with a combined standard uncertainty of 5 parts in  $10^3$ , consistent with the BIPM.RI(I)-K6 comparison results obtained in accelerator photon beams of the LNE-LNHB. It is also consistent with the BIPM.RI(I)-K4 comparison result obtained for the LNE-LNHB in the BIPM Co-60.

## 1. Introduction

In December 2010 the LNE-LNHB<sup>1</sup> made a request to participate with the BIPM in a bi-lateral comparison of absorbed dose to graphite in a Co-60 beam.

The BIPM has an ionometric primary standard for graphite but no comparisons in terms of absorbed dose to graphite have been undertaken since 2001. In the meantime, the BIPM has developed a graphite calorimeter standard for absorbed dose to water and since 2009 has carried out regular measurements using its graphite calorimeter in the CisBIO Co-60 reference beam at the BIPM. These are made as part of the quality assessment of the BIPM graphite calorimeter, but also with the objective to determine the absorbed dose to water in this beam. These calorimeter measurements can equally be used for the determination of the absorbed dose to graphite. In fact, the largest part of the information needed for a comparison in terms of absorbed dose to graphite was already available from these repeated measurements and the additional measurements required, namely ionometric measurements in a reference graphite phantom, would not be particularly time consuming. Further, such a comparison might give useful information on the advantages and limitations of the techniques applied in each laboratory. For this reason, a comparison of absorbed dose to graphite was undertaken.

Two comparison exercises were carried out. Firstly, a determination of absorbed dose to graphite was made by the LNHB in the BIPM reference beam using a LNHB transfer chamber in the BIPM graphite phantom. The BIPM reference beam is a collimated 10 cm × 10 cm square field for which the appropriate dose conversion was calculated using the BIPM phase-space files and geometries. Secondly, complementary measurements were carried out using a BIPM transfer chamber in the LNHB Co-60 reference beam. However, the LNHB beam has a circular profile and to determine the BIPM absorbed dose it would be necessary for the

---

<sup>1</sup> The LNE-LNHB will henceforth be referred to as the « LNHB ».

BIPM to calculate an appropriate conversion factor using the LNHB phase-space files and geometry. For this reason, only the results obtained at the BIPM have been exploited in this report.

The comparison result is represented by the ratio  $R$ ,

$$R = \frac{D_{G, \text{LNHB}}}{D_{G, \text{BIPM}}}, \quad (1-a)$$

and the associated combined relative standard uncertainty  $u_c$ ,

$$u_c \left( \frac{D_{G, \text{LNHB}}}{D_{G, \text{BIPM}}} \right). \quad (1-b)$$

The comparison measurements were carried out at the BIPM from 1 to 2 March 2011.

## 2. Method and Instrumentation

### 2.1. The LNHB determination of absorbed dose to graphite

The LNHB may realize absorbed dose using its primary standard in form of an originally designed graphite calorimeter [1 - 3]. The LNHB graphite calorimeter is associated with a homogeneous graphite phantom, consisting of set of well-characterized discs.

The LNHB graphite disc containing the ionization chamber in this work is of diameter 160 mm and 32 mm thick ("32a"). The disc contains a 10 mm diameter cavity in the radial direction into which a thimble-type ionization chamber is inserted. Note that measurements using this disc in its 'normal' orientation are corrected by the factor  $k_{\text{asym}}$  for any change in ionization current measured with the disc (but not the transfer chamber) reversed. A photograph of the LNHB graphite phantom is shown in Fig 1.

Before the comparison, measurements were carried out at the LNHB, using the LNHB graphite phantom, in which an ionization chamber (NE 2571, serial number 642)<sup>2</sup> was calibrated in terms of absorbed dose to graphite at the reference depth of 5 g cm<sup>-2</sup>. This chamber served as a transfer chamber in the comparison. The calibration factor and associated correction factors are listed in Table 1. The absorbed dose to graphite can hence be determined as

$$\dot{D}_G = N_{D,G} I_G \cdot \sum_i k_i. \quad (2)$$

---

<sup>2</sup> Certain commercial equipment, instruments, or materials are identified in this report in order to specify the experimental procedure adequately. Such identification is not intended to imply recommendation or endorsement by the participating institutes, nor is it intended to imply that the materials or equipment identified are necessarily the best available for the purpose.

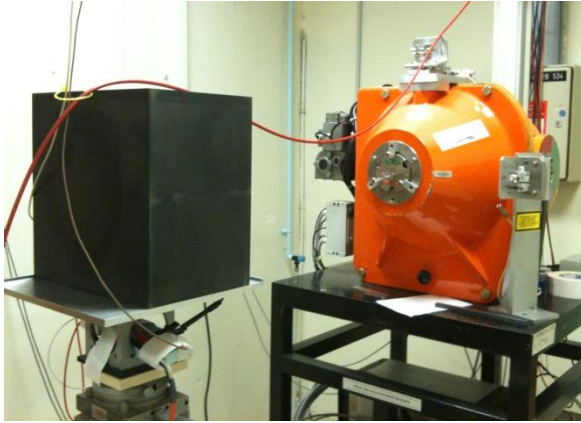


**Fig. 1.** Photograph of the LNHB graphite phantom placed in the LNHB Co-60 beam.

**Table 1.** Calibration coefficient for the NE 2571 transfer chamber (serial number 642) of the LNHB, corrected for the asymmetry of the disc containing the chamber ( $k_{asym}$ ), the polarity effect ( $k_{pol}$ ) and ion recombination ( $k_s$ ). The calibration coefficient is given for the reference conditions  $p=101.325$  kPa,  $T = 20.0$  °C and RH= 0 %.

Parameter	$y$	$[u(y)_c/y] / 10^{-3}$
$k_{asym}$	0.999 94	0.08
$k_{pol}$	0.998 83	0.33
$k_s$	1.001 19	0.50
$k_{rn}$	1.000 4	0.45
$N_{D,G} / [\text{Gy}\cdot\text{C}^{-1}]$	$3.983 \times 10^7$	2.56

## 2.2. The BIPM method to determine the absorbed dose to graphite

### 2.2.1. Measurement principle

The BIPM absorbed-dose graphite calorimeter is described in [4, 5]. No electrical heating is employed, but rather the specific heat capacity of the graphite core  $c_{p,c}$  has been determined previously in a separate experiment [6]. Quasi-adiabatic conditions are achieved by irradiating the core in a graphite jacket that is smaller than the radiation field, resulting in a relatively uniform dose distribution in the jacket. This arrangement is mounted in a PMMA<sup>3</sup> support and vacuum container with graphite

<sup>3</sup> Polymethylmethacrylate

build-up plates to centre the core at the reference depth of  $5 \text{ g cm}^{-2}$ . The mean absorbed dose  $D_c$  in the graphite core is determined using

$$D_c = c_{p,c}(T) \cdot \Delta T \cdot k_{\text{imp}}, \quad (3)$$

where  $\Delta T$  is the temperature rise in the core and  $k_{\text{imp}}$  corrects for non-graphite materials in the core.

Two nominally identical parallel-plate ionization chambers with graphite walls and collector, similar in design to the existing BIPM standards for air kerma and absorbed dose to water, were fabricated for the determination of the absorbed dose to graphite from the measured absorbed dose to the graphite core. The first chamber (calo 3) is housed in a graphite jacket, nominally identical to the calorimeter jacket, and is irradiated in the same PMMA support and phantom arrangement. The second chamber (calo5) is mounted in a large graphite phantom and irradiated with its centre at  $5 \text{ g cm}^{-2}$ . These measurement arrangements are represented schematically in Figure 2.

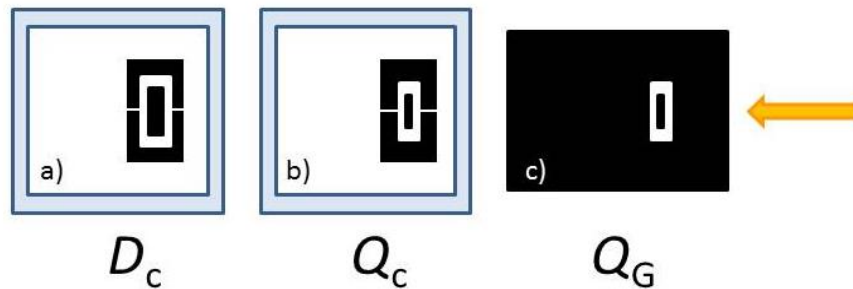


**Figure 2.** Schematic representation of the three measurement situations giving rise to Monte Carlo calculations; the yellow arrow indicates the incoming beam. Two of the measurements are made in a common cubic PMMA phantom. **a)** The calorimeter is used in vacuum and  $D_c$  is both measured and calculated. **b)** The graphite core is replaced by the transfer ionization chamber at atmospheric pressure. The ionization charge in graphite  $Q_c$  is measured and the corresponding cavity dose  $D_{\text{cav},c}$  calculated. **c)** The ionization chamber is placed in a large graphite phantom. The ionization charge in graphite  $Q_G$  is measured and the corresponding cavity dose  $D_{\text{cav},G}$  calculated. The mean absorbed dose to graphite  $D_G$  in the absence of the chamber is also calculated for a graphite detector with the same dimensions as the cavity. It follows that a correction factor  $k_{\text{rn}}$  is required for the radial non-uniformity of the radiation field over this dimension, measured for a homogeneous graphite phantom.

The method adopted by the BIPM combining calorimetric and ionometric measurements with Monte Carlo simulations to determine the absorbed dose to water is described in detail in [7] and has previously been applied for the determination of absorbed dose to water in [8-10]. In analogy, the absorbed dose to graphite  $D_G$  can be evaluated as

$$D_G = D_c \frac{Q_G}{Q_c} \left( \frac{D_G}{D_c} \right)^{MC} \left( \frac{D_{cav,c}}{D_{cav,G}} \right)^{MC} k_m, \quad (4)$$

where

- $D_c$  - measured absorbed dose to the graphite core;
- $Q_c$  - ionization charge measured when the transfer chamber is positioned in the graphite jacket, replacing the core;
- $Q_G$  - ionization charge measured when the transfer chamber is positioned in the graphite phantom;
- $\left( \frac{D_G}{D_c} \right)^{MC}$  - calculated ratio of absorbed dose to the graphite phantom and to the graphite core using Monte Carlo simulations;
- $\left( \frac{D_{cav,c}}{D_{cav,G}} \right)^{MC}$  - calculated ratio of cavity doses in the two graphite arrangements using Monte Carlo simulations;
- $k_m$  - measured correction for radial non-uniformity in graphite.

In abbreviated form,  $D_G$  can be expressed as

$$D_G = D_c \frac{Q_G}{Q_c} C_{G,c} k_m, \quad (5)$$

where  $C_{G,c}$  represents the total Monte Carlo conversion factor.

### 2.2.2. Monte Carlo simulations

The Monte Carlo calculations are described in detail in [7] and make use of the PENELOPE code [11]. As noted in the preceding section, four geometries are simulated and the accuracy of the method relies on the symmetry of the geometries and the simulation parameters. A novel aspect of this is the use of a disc-shaped transfer chamber whose total graphite thickness on-axis is the same as that of the calorimeter core. Very few of the geometrical bodies appear in only one of the four simulations so that the fine details should not need to be simulated. Nevertheless, a very detailed geometrical model was constructed. Similarly, although detailed electron transport should not be essential for the same reasons, sufficient detail was used to permit the cavity dose to be calculated in a way that gives the same results as a full calculation using event-by-event electron transport (as demonstrated in an earlier work [12]). Reference [7] includes a detailed uncertainty analysis for the calculation of the conversion factor  $C_{w,c}$  for the determination of absorbed dose to water.

Phase-space files of incident photons at 90 cm from the BIPM Co-60 source have earlier been generated using the PENELOPE code [11, 13]. In total,  $2.5 \times 10^7$  independent photons are available, distributed for convenience in 24 files. The phase-space files have here been used to calculate  $C_{G,c}$  rather than  $C_{w,G}$ .

The result of the calculations for  $C_{G,c}$  is listed in Table 3. The figures in parentheses represent the combined standard uncertainty in the trailing digits based on the analysis for  $C_{w,c}$  presented in [7], including components arising from the simulation geometries, input spectra, radiation transport mechanisms and cross-section data used. The value is slightly reduced from the 1.7 parts in  $10^3$  given in [7] because the ratio of photon cross sections for water and graphite does not enter into the present work. The statistical standard uncertainty for  $C_{w,c^2}$  is around 0.03 %.

### 2.2.3. BIPM Graphite Phantom

The BIPM graphite phantom was constructed in 1973 and consists of seven stacked graphite discs 300 mm in diameter. The density of the discs fabricated at that time varied within 1.2 % [14] but local density variations within one single disc were sometimes larger than 2 % [15]. For this reason, the centre of each disc was compared to a sample of known density to decrease the associated uncertainty contribution [16]. A cylindrical hole allowed the front graphite disc to house a primary standard parallel-plate ionization chamber. cf. Figs 3-a and 3-b.

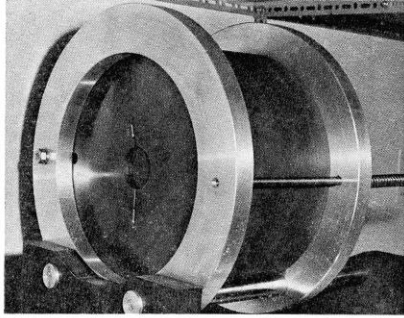


Fig. 11. — Fantôme de graphite pour la mesure de la dose absorbée.

Le premier disque a été enlevé pour permettre de voir le logement de la chambre à cavité.

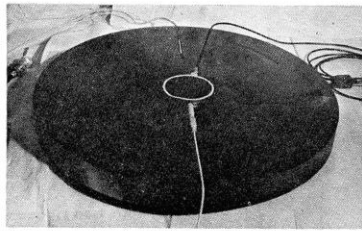


Fig. 12. — Premier disque du fantôme avec la chambre à cavité et la thermistance.

**Fig. 3-a** Photographs of the BIPM graphite phantom in 1973 where the first disc, facing the beam, has been removed (*Fig. 11 in the photograph*) to show the rear of the disc housing the parallel-plate ionization chamber (*Fig. 12 in the photograph*) [14].



**Fig. 3-b** Photograph of the BIPM graphite phantom placed in the BIPM CisBIO Co-60 beam in 2011.

However, for the present comparison, a specially-adapted graphite disc was fabricated to house a newly-constructed parallel-plate ionization chamber {f} (calo5) with well-known cavity volume<sup>4</sup>. The dimensions of this “inner” disc {c} (160 mm diameter, 32 mm thick) were chosen to be similar to the LNHB phantom centre plate with the aim of using it with both the BIPM and LNHB phantoms. To centre this disc in the BIPM phantom, a pre-existing graphite ring 30 mm in diameter {d}, and a 2 mm thick PMMA ‘spacer’ ring {e} were placed around the inner disc. The front face of the ionization chamber is recessed from the front face of the

<sup>4</sup> The letters {a}, {b}, {c} etc. refer to the information given in Table 2.

disc. To fill this space, a graphite cylinder {b} of well-known bulk density is placed so that it is coplanar with the front face of the disc.

### 2.3. Configuration for the LNHB-BIPM Comparison.

To compare the determination of absorbed dose to graphite by the LNHB and the BIPM, two graphite phantom configurations were used. Firstly, the LNHB 160 mm diameter, 32 mm thick disc ("32a") {g} was incorporated into the BIPM graphite phantom as described in 2.2.3, cf. Fig. 4. Measurements were made in this configuration using the LNHB ionization chamber (NE 2571, serial number 642). Secondly, the BIPM 160 mm diameter, 32 mm thick disc was housed in the BIPM graphite phantom, cf. Fig. 5. Measurements were made in this configuration using the BIPM ionization chamber (calo5). The bulk density and mass-thickness of the components are listed in Table 2.

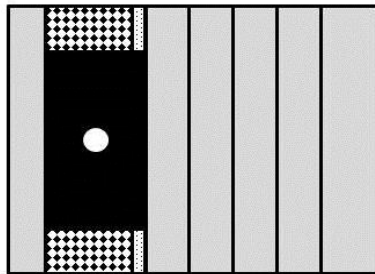


**Fig. 4** BIPM graphite phantom housing the LNHB graphite disc. The checked area corresponds to an outer graphite ring.

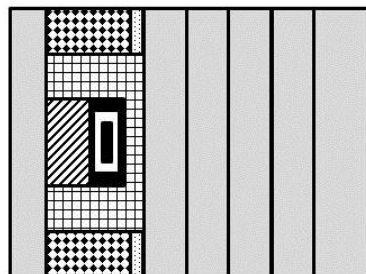


**Fig. 5** BIPM graphite phantom housing the parallel plate ionization chamber 'calo5'. The checked area corresponds to an outer graphite ring.

**Table 2.** Components of the phantom assembly upstream the measurement plane. The density  $\rho$  and mass thickness  $d_m$  of graphite phantom components used in the comparison are given for the components in the centre of the beam.

component	symbol	$\rho / \text{g cm}^{-3}$	$d_m / \text{g cm}^{-2}$
{a} front disc in graphite		1.741	2.006
{b} BIPM small graphite cylinder		1.814	2.359
{c} BIPM inner graphite cylinder		1.814	1.438
{d} graphite ring		–	–
{e} PMMA ring		–	–
{f} BIPM ionization chamber, cf. Fig5		1.834	1.015
{g} LNHB inner graphite cylinder, cf. Fig.4		1.837	2.939

The BIPM ionization chamber was placed in a so called ‘compensated’ configuration, i.e. the total mass thickness of graphite on the central beam axis from the front face to the centre of the chamber collector constitutes  $4.998 \text{ g cm}^{-2}$  (nominal value:  $5 \text{ g cm}^{-2}$ ). The mass thickness upstream of the LNHB ionization chamber was  $4.945 \text{ g cm}^{-2}$ , numerically close to the BIPM mass thickness, but in a so called ‘non-compensated’ configuration for which the chamber air cavity is considered to be graphite<sup>5</sup>. This results in slightly different SSDs<sup>6</sup>, as schematized in Fig 6.

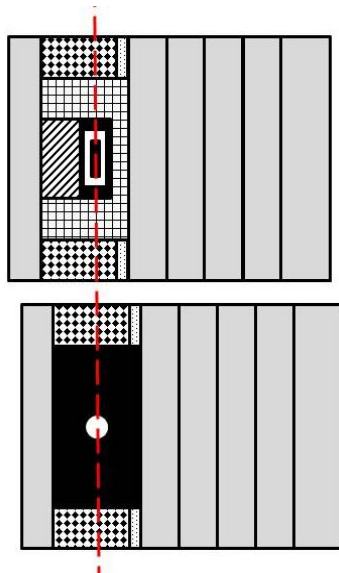


**Fig. 6** Illustration of the relative positioning of the BIPM (upper) and LNHB (lower) configurations. The red dashed line indicates the detector plane. The front faces are ‘misaligned’ by around 2 mm.

<sup>5</sup> There is no clear advantage of one method over the other. What is important for the present comparison is that the Monte Carlo calculations for the BIPM standard replicate the compensated mode and determine the absorbed dose under the non-compensated conditions used for the LNHB ionization chamber.

<sup>6</sup> Source to Surface Distance

### 3. Measurement Results and Discussion

#### 3.1. Measurement Results

The results obtained using the BIPM calorimeter and calo5 ionization chamber are listed in Table 3. The parameters  $\dot{D}_c$  and  $I_c$  are the result of many repeat measurements in the small calorimeter phantom (Figs. 2(a) and 2(b), respectively) between 2009 to 2012 (including measurements made after the present comparison). The parameter  $I_G$  represents the current measured for this comparison in the large phantom (Fig. 5) at a mass thickness of  $4.998 \text{ g cm}^{-2}$  in compensated mode. The difference between these conditions for  $I_G$  and the non-compensated conditions used for the LNHB ionization chamber (Fig. 4) is accounted for by the Monte Carlo factor  $C_{G,c}$  in the table. Using (5), the absorbed dose rate to graphite  $\dot{D}_{c,BIPM}$  in the CisBIO Co-60 beam at 2011-01-01 00:00:00 UTC and at the reference depth of  $4.945 \text{ g cm}^{-2}$  (non-compensated) is determined as

$$\dot{D}_{c,BIPM} = 5.333 \text{ mG y}\cdot\text{s}^{-1} \quad (7)$$

with an associated relative standard uncertainty of 3.6 parts in  $10^3$ .

**Table 3.** Measured or calculated parameters used to determine the absorbed dose to graphite in the BIPM Co-60 reference beam using the BIPM calorimeter.

Parameter	$y$	$[u(y)/y] / 10^{-3}$
$\dot{D}_c / [\text{Gy}\cdot\text{min}^{-1}]$	0.2968	1.5
$I_c / \text{pA}^7$	1286.8	0.5 <sup>8</sup>
$k_{m,G} [17]$	1.0032	1.0
$C_{G,c}$	1.0080	1.4
$I_G / \text{pA}^7$	1371.8	0.5 <sup>8</sup>
$d_m / [\text{g}\cdot\text{cm}^{-2}]$	4.998	0.4

<sup>7</sup> Corrected for volume, orientation and polarization.

<sup>8</sup> Uncertainty of positioning included in the estimate.

The LNHB disc housing the transfer ionization chamber (serial number 642) was placed in the BIPM graphite phantom, replacing the corresponding BIPM disc (Fig.5). The results obtained for the LNHB transfer chamber at the BIPM are given in Table 4. A decay correction has been included to compare the data on 2008-01-01 (using the same Co-60 half-life for the LNHB and BIPM determinations). Further, the BIPM measurement system gives currents normalized to 0° C and for a relative humidity of 50 %, giving rise to two supplementary corrections.

**Table4.** Measured or calculated parameters used to determine the absorbed dose to graphite in the BIPM Co-60 reference beam using the LNHB transfer chamber. The calibration coefficient  $N_{Dc}$  for the transfer chamber is given for the reference conditions  $p = 101.325$  kPa,  $T = 20.0$  °C and RH= 0 %, and consequently the ionization current  $I_c$  measured at the BIPM is normalized to these conditions. Correction factors are applied for the asymmetry of the LNHB disc ( $k_{asym}$ ), polarity ( $k_{pol}$ ), recombination ( $k_s$ ), radial non-uniformity ( $k_{rn}$ ) and source decay ( $k_{decay}$ ).

Parameter	$y$	$[u(y)_c/y] / 10^{-3}$
$N_{Dc} / [\text{Gy}\cdot\text{C}^{-1}]$	$3.983 \times 10^7$	2.56
$I_c / \text{pA}$	142.87	0.1
$k_T$	0.9318	0.2
$k_{RH}$	0.997	0.3
$k_{asym}$	0.999 94	0.08
$k_{pol}$	0.998 83	0.33
$k_s$	1.001 19	0.50
$k_{rn,c}$	1.000 5	0.1
$\dot{D}_c / [\text{Gy}\cdot\text{min}^{-1}]$	5.289	2.6

Using (2), the LNHB determination of absorbed dose rate to graphite  $\dot{D}_{c,LNHB}$  in the CisBIO Co-60 beam at 2011-01-01 00:00:00 UTC and at the reference depth of  $4.945 \text{ g cm}^{-2}$  (non-compensated) is determined as

$$\dot{D}_{c,LNHB} = 5.289 \text{ mG y}\cdot\text{s}^{-1} \quad (8)$$

with an associated relative standard uncertainty of 2.6 parts in  $10^3$ .

### 3.2. Comparison Result and Discussion

From (7) and (8) the comparison result is derived as

$$A = \frac{D_{c, \text{LNHB}}}{D_{c, \text{BIPM}}} = 0.992, \quad (9)$$

with a combined relative standard uncertainty  $u_c$  of 5 parts in  $10^3$ .

While the LNHB and BIPM standards agree at around 1.5 times the standard uncertainty of the comparison, there are several factors that complicate the comparison and might result in small differences between the determinations of absorbed dose to graphite.

The use of composite graphite phantoms containing a chamber holder, outer supporting rings and build-up plates with different bulk densities presents a particular difficulty for comparisons in terms of absorbed dose to graphite in the sense that, for a phantom and field size of given dimensions, the absorbed dose is not uniquely specified by the reference depth expressed in  $\text{g cm}^{-2}$ . One can see this qualitatively by recognizing that increasing the bulk density effectively increases the amount of material irradiated laterally and might therefore produce an effect similar to increasing the field size. The effect for a composite phantom is less easy to predict. Monte Carlo calculations were made at  $5 \text{ g cm}^{-2}$  for a homogeneous phantom with bulk density  $1.78 \text{ g cm}^{-2}$  and for a composite phantom where the first  $2 \text{ g cm}^{-2}$  of build-up is a plate with density  $1.74 \text{ g cm}^{-2}$  (similar to disc {a} in Figs. 4 and 5) and the chamber holder (making up the next  $3 \text{ g cm}^{-2}$  and beyond) has density  $1.84 \text{ g cm}^{-2}$  (similar to disc {g} in Fig. 4). These show the absorbed dose for the composite phantom to be higher by 0.3 %, a surprisingly large effect for the realistic variations in bulk density simulated.

Furthermore, the mean bulk density measured (and simulated) for a given graphite component might not be a sufficiently good representation, especially if local inhomogeneities exist and in particular for the upstream graphite components close to the beam axis. The fact that the LNHB and BIPM transfer chambers are very different in cross section might also be relevant (aside from the first-order effect correct by  $k_{rn}$ ). The magnitude of these effects and the associated uncertainty are difficult to estimate but might be possible to evaluate using a similar technique to that of Boutillon [16]. These effects represent a significant limitation when measuring absorbed dose to graphite.

To best take account of this in the present comparison, the BIPM absorbed-dose conversion from  $D_c$  (the measured dose to the calorimeter core in its small phantom, i.e. jacket) to  $D_G$  (the dose estimate used for the comparison), was calculated for the precise conditions of irradiation of the BIPM and LNHB chambers. In other words, the cavity dose  $D_{cav,G}$  was calculated for the composite phantom used for the BIPM chamber, while  $D_G$  was calculated for the phantom used for the LNHB transfer chamber (replacing the chamber itself by graphite of the same density as the chamber holder). By adopting this method, any remaining errors are expected to be below 0.1 % and an additional uncertainty of this value is included. Note that by using this method, slight deviations of the chamber depths from  $5 \text{ g cm}^{-2}$  are taken into account and no depth corrections need be applied.

A BIPM.RI(I)-K6 comparison of calorimetric determinations of absorbed dose to water in accelerator photon beams was carried out between the LNHB and the BIPM in March 2012 [18]. For these beams, the BIPM standard is the same graphite calorimeter; however, for the LNHB the high-energy standard is a combination of results based on graphite and water calorimeters. The present result is in consistency with the results of the comparison between the two laboratories at 6 MV and 20 MV, determined at 0.995 and 0.994, respectively, with a combined standard uncertainty of 5 parts in  $10^3$ . Meanwhile, the absorbed dose to water determined using the BIPM ionometric standard has been compared in the BIPM Co-60 reference beam with that determined using the BIPM graphite calorimeter system. The ratio of these determinations has been evaluated as 0.9995(25) [19]. As a consequence, the result presented in this report is also consistent with the result of the BIPM.RI(I)-K4 [20].

#### 4. Conclusion

A comparison of absorbed dose to graphite in a Co-60 reference beam was carried out between the Laboratoire National de Métrologie et d'Essais - Laboratoire National Henri Becquerel (LNE-LNHB) and the Bureau International des Poids et Mesures (BIPM) in March 2011. The comparison involved the LNE-LNHB primary standard graphite calorimeter and the BIPM graphite calorimeter used for the BIPM.RI(I)-K6 comparison of national accelerator beam facilities. The comparison result, reported as a ratio of the LNE-LNHB and the BIPM evaluations, is 0.992 with a combined standard uncertainty of 5 parts in  $10^3$ . This result is in consistency with the results of the comparison between the two laboratories for absorbed dose to water in accelerator photon beams [18], where a ratio of the LNE-LNHB and the BIPM evaluations at 6 MV was determined at 0.995 with a combined standard uncertainty of 5 parts in  $10^3$ . It is also consistent with the result of the BIPM.RI(I)-K4 [20].

## References

- [1] Daures J, Chauvenet B and Ostrowsky A 1994 State-of-the-art of calorimetry at LPRI *Proc. NPL Calorimetry Workshop 1994 (National Physical Laboratory, Teddington, UK)*
- [2] Daures J, Ostrowsky A, Gross P, Jeannot J P and Gouriou J 2000 Calorimetry for absorbed dose measurements at BNM-LNHB *Proc. NPL Workshop on Recent Advances in Calorimetric Absorbed dose Standards, NPL Report CIRM-42*
- [3] Daures J and Ostrowsky A 2005 New constant-temperature operating mode for graphite calorimeter at LNE-LNHB *Phys. Med. Biol.* **50** 4035
- [4] Picard S, Burns D T and Roger P 2009 Construction of an Absorbed-Dose Graphite Calorimeter [\*Rapport BIPM-2009/01\*](#) (Sèvres: Bureau International des Poids et Mesures) 12 pp.
- [5] Picard S, Burns D T, Roger P 2010 The BIPM Graphite Calorimeter Standard for Absorbed Dose to Water, abstract to International Symposium on Standards, Applications and Quality Assurance in Medical Radiation Dosimetry *in Standards, Applications and Quality Assurance in Medical Radiation Dosimetry (IDOS), 2011, vol. 1* 55–65, Proceedings Series – International Atomic Energy Agency 2011.
- [6] Picard S, Burns D T and Roger P 2007 Determination of the Specific Heat Capacity of a Graphite Sample Using Absolute and Differential Methods [\*Metrologia\* \*\*44\*\* 294–302](#)
- [7] Burns D T 2011 The dose conversion procedure for the BIPM graphite calorimeter standard for absorbed dose to water, in preparation.
- [8] Picard S, Burns D T, Roger P, Allisy-Roberts P J, McEwan M, Cojocaru C, Ross C 2010 Comparison of the standards for absorbed dose to water of the NRC and the BIPM for accelerator photon beams [\*Metrologia\* \*\*47\*\* Tech. Suppl. 06025](#), 22 pp.
- [9] Picard S, Burns D T, Roger P, Allisy-Roberts P J, Kapsch R P and Krauss A 2011 Key comparison BIPM.RI(I)-K6 of the standards for absorbed dose to water of the PTB, Germany and the BIPM in accelerator photon beams [\*Metrologia\* \*\*48\*\* Tech. Suppl. 06020](#), 21 pp.
- [10] Picard S, Burns D T, Roger P, Bateman F B, Tosh R E, Chen-Mayer H 2012 Key comparison BIPM.RI(I)-K6 of the standards for absorbed dose to water of the NIST, USA and the BIPM in accelerator photon beams [\*Metrologia\* \*\*50\*\* Tech. Suppl. 06004](#), 22 pp.
- [11] Salvat F, Fernandez-Varea J M and Sempau J 2009 PENELOPE-2008: A code system for Monte Carlo simulation of electron and photon transport *NEA No. 6416 Workshop Proc. (Barcelona, Spain 30 June – 3 July 2008)* (Paris: NEA/OECD)
- [12] Burns D T 2006 A new approach to the determination of air kerma using primary-standard cavity ionization chambers *Phys. Med. Biol.* **51** 929–942
- [13] Burns D T 2003 Calculation of k<sub>air</sub> for <sup>60</sup>Co Air-Kerma Standards Using PENELOPE [\*CCRI\(I\)/03–40\*](#) (Sèvres: BIPM)
- [14] *Procès-Verbaux des Séances du Comité International des Poids et Mesures*, 62nd meeting (1973) 63-65.
- [15] *Procès-Verbaux des Séances du Comité International des Poids et Mesures*, 63rd meeting (1974) 59-60.

- [16] *Comité Consultatif pour les Etalons de Mesure des Rayonnements Ionisants Section I. – Rayons X et  $\gamma$ , electrons. Report of the 3rd meeting (1975) RI(I) 61.*
- [17] Boutillon M 1981 Determination of absorbed dose in a water phantom from the measurement of absorbed dose in a graphite phantom [\*Rapport BIPM-1981/2\*](#) (Sèvres: Bureau International des Poids et Mesures) 6 pp.
- [18] Picard S, Burns D T, Roger P, Delaunay F, Le Roy M, Ostrowsky A, Sommier L, Vermesse D 2013 Key comparison BIPM.RI(I)-K6 of the standards for absorbed dose to water of the LNE-LNHB, France and the BIPM in accelerator photon beams [\*Metrologia 50 Tech. Suppl. 06015\*](#), 24 pp.
- [19] Burns D T, Picard S, Kessler C and Roger P 2013 Comparison of the BIPM ionometric and calorimetric  $D_w$  standards for  $^{60}\text{Co}$ , Consultative Committee for Ionizing Radiation, Section I, working document CCRI(I)/13-20 3 pp.
- [20] C Kessler<sup>1</sup>, D T Burns<sup>1</sup>, F Delaunay<sup>2</sup> and M Donois 2013 Key comparison BIPM.RI(I)-K4 of the absorbed dose to water standards of the LNE–LNHB, France and the BIPM in  $^{60}\text{Co}$  gamma radiation [\*Metrologia 50 Tech. Suppl. 06019\*](#), 11 pp.